Core-shell spheres for ELM tuning and quantitative impurity physics

Zhehui Wang[1,*], Jiansheng Hu[2], Shengtai Li[1], Rajesh Maingi[3], Zhen Sun[2], Jonathan Menard[3], John A. Oertel[1], Xuan Sun[4], X. Q. Xu[5], Guizhong Zuo[2]

[1] *Los Alamos National Laboratory, Los Alamos, NM 87545, USA*

[2] *Institute of Plasma Physics, Chinese Academy of Sciences, Hefei, AH 230031, China*

[3] *Princeton Plasma Physics Laboratory, Princeton, NJ 08544, USA*

[4] *University of Science and Technology of China, Hefei, AH 230026, China*

[5] *Lawrence Livermore National Laboratory, Livermore, CA 94550, USA*

Abstract

In addition to supplying sensitive real-time imaging and spectroscopy information about impurity physics, unique features of core-shell spheres of impurity atoms are discussed for ELM tuning in magnetic fusion. Examples of core-shell spheres, including balloon-like structures, are given. Further development of core-shell spheres and their experimental implementation in EAST, NSTX-U are planned.

Introduction

One approach to heat flux control in burning plasmas is through edge localized mode (ELM) tuning, which includes both ELM pacing and ELM suppression. ELM pacing is to induce ELMs at a frequency higher than that of natural ELMs, so that the instantaneous heat flux onto the divertor and other plasma facing components can be kept as low as possible while maintaining or maximizing time-averaged heat flux released from the plasma core. Fueling pellets of cryogenic deuterium as well as impurity pellets other than cryogenic deuterium have been experimentally shown to be promising for ELM tuning.

ELM pacing and suppression have recently been observed in the EAST tokamak using lithium granules ('larger pellets of mm sizes') and lithium powder ('smaller pellets of sub-mm sizes'). In the EAST experiment, ELM pacing is associated with larger lithium pellets while ELM suppression is associated with injection of lithium powder. The physical mechanisms of ELM pacing and suppression are related to each other. ELM pacing is to enhance the local plasma density and pressure to above the ballooning instability threshold, while ELM suppression is through smoothing of the local plasma density and pressure profile. Quantitative understanding of ELM pacing and suppression are being pursued using sophisticated MHD calculations.

*Correspondence: zwang@lanl.gov

One potential concern with ELM tuning using impurity pellets is plasma core contamination. Low-Z ions of lithium, similar to hydrogen (Z/A=1/1), helium, boron, carbon, *etc.*, may be fully striped of electrons and therefore does not cause radiative cooling directly. However, they can take up a fraction plasma beta and cause loss of hot fusion ions through charge exchange. High-Z ions such as tungsten, however, can cause significant radiative cooling if they migrate inside the separatrix or reach the plasma core.

Compared with conventional pellets that have uniform material composition and density throughout the volume of a pellet, a core-shell sphere have radially dependent material compositions or mass densities that allow precise control of impurity release in plasmas and therefore a variety of new magnetic fusion applications. Core-shell structured impurity spheres can be used for ELM tuning while reducing the probability of plasma contamination. Core-shell spheres can also be used to examine pellet ablation physics quantitatively and to study real-time impurity transport by supplying precise spectroscopy information. Some examples of core-shell spheres are given. Core-shell spheres are being considered for the upcoming experiments on EAST, NSTX-U, and elsewhere.

Core-shell sphere ablation in high-temperature plasmas

Similar to the cryogenic pellet ablation, impurity pellet ablation is regulated by ablated neutral gas shielding (NGS). Meanwhile, higher ablation energy per atom leads to a transient neutral gas cloud that reduces the plasma heating (dominated by electrons) to a much less extent than in the case of cryogenic pellets. The neutral gas cloud density profile is determined by two parameters [3]: ξ, the plasma heating to cloud expansion cooling ratio, and γ, the ratio of the specific heat. We will use $\gamma = 5/3$ for boron, lithium and other impurities. ξ is in the range of $\sim$10 to a few 10^3 for many plasmas including EAST. Until recently [1], impurity pellet injection has been mostly avoided in high-temperature magnetic fusion plasmas. Therefore, more experimental data are needed to de-

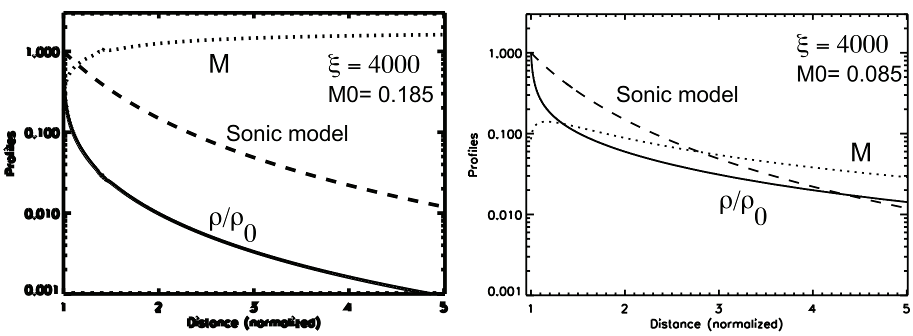

Figure 1: *(Left) Gas dynamic model prediction of sonic transition for sufficiently large ξ (=4000) and the gas flow speed leaving the pellet surface at 0.185$\times$the local sound speed. (Right) The same model gives subsonic flow and a different density profile when the initial gas flow velocity is smaller.*

veloping theoretical models for impurity ablation. Meanwhile, a number of other factors also limit the efficacy of the theoretical models. The first factor is the lack of the electron stopping power data in materials such as boron, lithium; in particular, for the electron energy in the range of 10 eV to 10 keV. The problem may be unique to plasmas since the gaseous forms of boron and lithium may only exist in a high-temperature plasma environment for a short period of time. The second factor is that theoretical predictions of pellet ablation are sensitive to boundary conditions. Two examples are given in Fig. 1 for different gas flow speeds at the pellet surface. For a sufficiently fast gas flow, the familiar sonic transition is expected. For sufficiently small gas flow speed, however, the sonic transition may never happen.

Core-shell structured pellets can be used to resolve the theoretical uncertainties and may also supply experimental to expand the database for electron stopping power. A simple layered core-shell structure will allow us to measure the ablation rate dr_p/dt directly based on distinctive characteristic optical emissions from different layers. For a 2-mm diameter micropellet, a thin layer of 10 μm lithium corresponds to 5.6×10^{18} lithium atoms on the surface. The mean electron energy arriving at the pellet surface can be estimated by the time to ablate away a certain layer thickness. Electron range in the lithium layer is about 8.6 nm for 100 eV electrons, and 0.14 μm for 1 keV electrons. The time duration to fully ablate away a certain layer thickness is inversely proportional to the average electron energy; *i.e.*, for similar electron fluxes, it would take about 10 times longer for 100 eV electrons than for 1 keV electrons.

Time-dependent imaging & spectroscopy signatures

Core-shell pellets offer time-dependent optical emission signatures for imaging and spectroscopy [2]. In a 1 keV plasma with a density of 10^{19} m^{-3}, the time to ablate through a 10 μm thin lithium shell is about 6 μs when there is no shielding effect. Shielding effect will increase the ablation time in proportion. The existing imaging cameras can be used to measure the duration of ablation. Fig. 2 shows an ablation movie of a lithium granule (with conventional solid structure) using a Phantom 710 camera (8-bit, Vision Research). Except in the last frame (bottom right), where the bright 'cigar'-like cylindrical column saturates the camera, two key features stand out in other frames: the bright circular core and the elongated oval-

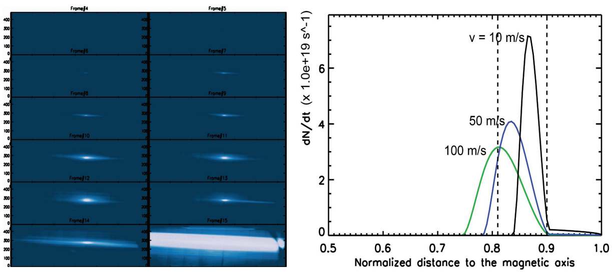

Figure 2: *(Left) A lithium granule (85 m/s) ablation as function of time (640×480 pixel format). (Right) Explanation of the rapid transition from a tenuous light emission mode to an intense emission mode.*

shaped periphery surrounding the core. The core region is dominated by the ablated neutral gaseous lithium atoms, estimated to be 14.4 mm in diameter, or about 20$\times$ the original lithium granule diameter (0.7 mm) based on electron impact ionization. The neutral atoms in the core are not affected by the magnetic field (therefore circular). The periphery corresponds to the cloud of ionized lithium, which follows the magnetic field line when expanding near the local sound speed of 1.8 km/s, or 9.5 cm (19 kfps frame rate) with a motional blur of 1.8 cm (10 μs exposure time). The sudden increase in brightness in the bottom right frame is attributed to the transition from a relatively cold edge plasma to the pedestal or further inside the separatrix, when both electron density and temperature increase drastically. The ablation rate or the ξ parameter is also expected to increase dramatically. Correlated plasma density and temperature will be needed to make the model more quantitative. Utilization of spectral line filters will allow us to distinguish between neutrals and ions better.

A note on core-shell spheres

We are interested in core-shell spheres greater than 1 μm and less than $\sim$ 1 cm for ELM tuning and impurity physics. The lower limit is related to sensitivity for imaging and spectroscopy. The upper limit is related to the amount mass perturbation tolerable to high-temperature plasmas. We also mention here that for disruption mitigation, hollow spheres >1 cm may be useful as well. Micrometer core-shell spheres have been developed for chromatography [4]. There are a number of core-shell particles commercially available, some brands (vendors) include Poroshell (Agilent), Halo (Advanced Materials Technology), Cortecs (Waters), Kinetex (Phenomenex) and Accucore (Thermo Fisher Scientific). One of the issues with the existing commercial suppliers of core-shell spheres is their compatibility with the requirements of burning plasmas. A collaboration with chemists and material experts would be valuable for tailored core-shell spheres.

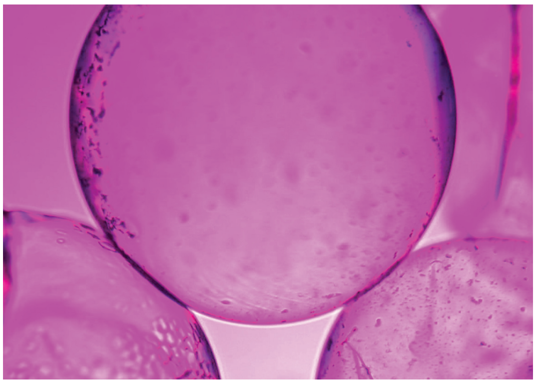

Figure 3: *Examples of 'balloon'-like hollow spheres made of polystyrene. The diameter is about 2 mm.*

References

[1] Z. Wang, R. Lunsford, D. K. Mansfield and J. H. Nichols, *J. Plasma Phys.* **82**, (2016) 615820202.

[2] Z. Wang, Q. Liu, W. Waganaar, J. Fontanese, D. James and T. Munsat, *Rev. Sci. Instrum.* **87**, (2016) 11D601.

[3] S. L. Milora and C. A. Foster, *IEEE Trans. Plasma Sci.* **PS-6** (1978) 578.

[4] R. Hayes, A. Ahmed, T. Edge and H. Zhang, *J. Chrom. A.* **1357** (2014) 36-52.